


PAPER

View Article Online
View Journal | View Issue

Building new discrete supramolecular assemblies through the interaction of iso-tellurazole N-oxides with Lewis acids and bases†

Peter C. Ho, Hilary A. Jenkins, James F. Britten and Ignacio Vargas-Baca *

Received 21st February 2017, Accepted 7th April 2017

DOI: 10.1039/c7fd00075h

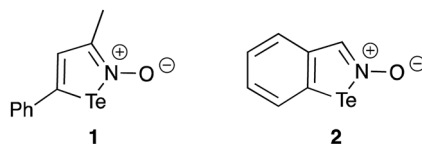
The supramolecular macrocycles spontaneously assembled by iso-tellurazole N-oxides are stable towards Lewis bases as strong as N-heterocyclic carbenes (NHC) but readily react with Lewis acids such as BR_3 ($\text{R} = \text{Ph}, \text{F}$). The electron acceptor ability of the tellurium atom is greatly enhanced in the resulting O-bonded adducts, which consequently enables binding to a variety of Lewis bases that includes acetonitrile, 4-dimethylaminopyridine, 4,4'-bipyridine, triphenyl phosphine, a N-heterocyclic carbene and a second molecule of iso-tellurazole N-oxide.

Introduction

The ability of σ -hole interactions – most prominently halogen bonding – to influence molecular organization and the properties of crystalline solids is now well established.^{1–4} This phenomenon has been successfully applied in other macroscopic assemblies such as liquid crystals.⁵ Attention is now turning to the other extreme of size, *i.e.* discrete assemblies of a few molecules with well-defined structures, properties and function. Significant recent developments in this area include the demonstration of anion recognition by rotaxanes,^{6,7} bis-tellurophenes,⁸ and chelating antimony(III) receptors;⁹ the creation of organocatalysts based on halogen¹⁰ and chalcogen bonding;¹¹ the construction of halogen-bonded molecular capsules¹² and functional macrocycles self-assembled by chalcogen bonding.¹³ In the last example, molecules of iso-tellurazole N-oxides such as **1** (Scheme 1), undergo reversible autoassociation through $\text{Te}\cdots\text{O}$ interactions into annular structures (**1₄**, **1₆**, Scheme 2) that are persistent in solution and function

Department of Chemistry and Chemical Biology, McMaster University, 1280 Main Street West, Hamilton, Ontario, Canada L8S 4M1. E-mail: vargas@chemistry.mcmaster.ca

† Electronic supplementary information (ESI) available: DFT-optimised structures. CCDC 1532977, 1532984, 1532985, 1532987, 1532988, 1532989, 1532990, 1532991 and 1532996. For ESI and crystallographic data in CIF or other electronic format see DOI: 10.1039/c7fd00075h



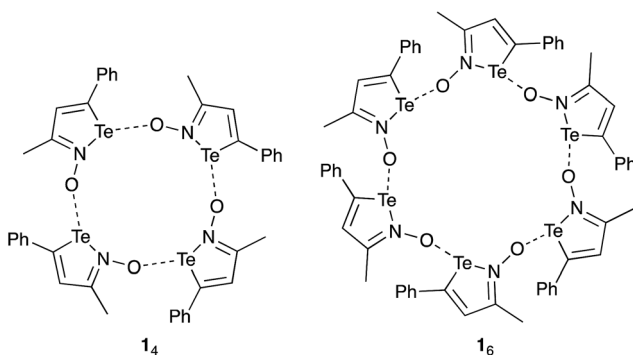
Scheme 1 Iso-tellurazole N-oxides in this study.

as actual macrocycles able to complex transition metal ions, form adducts with fullerenes, and host small molecules.

Remarkably for molecules with Te–N bonds, these heterocycles and their aggregates are stable in ambient conditions and are tolerant of water. Mineral acids such as HX (X = Cl, Br) protonate the oxygen atom while the halide binds the chalcogen atom yielding X–1–H.¹⁴ The process is reversible and is applicable to switching on and off the self-assembly of macrocycles. One of the limitations of these systems is their laborious syntheses which require several steps under an inert atmosphere. In this regard, the benzoannulated derivative 2 (ref. 15) is more convenient because its synthesis is simpler while it displays the same ability to assemble macrocyclic tetramers and hexamers.

Sigma-hole bonding is a particular case of the Lewis acid–base concept. Halogen-bonding acceptors are Lewis bases, and halogen-bonding donors are Lewis acids. Amphiphilic molecules like 1 and 2 that undergo autoassociation are in effect Lewis pairs. Compounds such as 1,2,5-chalcogenadiazoles are so strongly associated in the solid state that coordinating solvents such as pyridine or dimethylsulfoxide are required to dissolve them and, in some instances, it is possible to isolate the corresponding adducts.¹⁶ Several reports have examined in detail the binding of such heterocycles to neutral and anionic Lewis bases in the solid state^{17–19} and in solution.²⁰

In this report we examine the interaction of Lewis acids and bases with 1 and 2 to establish in which conditions the Te...O chalcogen bonds are disrupted and whether that process can be exploited in the construction of new discrete supramolecular assemblies. As the end goal is preparative, here we only present products that could be isolated as crystalline solids and thus structurally characterised by X-ray diffraction. The Lewis acids in this case are the boranes BPh₃



Scheme 2 Macrocytic aggregates of 1.

and BF_3 . The bases include acetonitrile, 4-dimethylamino-pyridine (DMAP), 4,4'-bipyridine (4,4'-bipy), triphenyl-phosphine, and the N-heterocyclic carbene 1,3-bis(2,6-diisopropylphenyl)-1,3-dihydro-2*H*-imidazol-2-ylidene (**3**).

Results and discussion

Spectroscopic and synthetic investigations

In room-temperature experiments, the resonances in the ^1H NMR spectra of **1** and **2** exhibited only small changes of position ($<3 \times 10^{-4}$ ppm) upon mixing with a stoichiometric amount of each Lewis base (Fig. S1†). Frequency shifts of comparable magnitude were observed when the solution NMR spectrum of pure iso-tellurazole N-oxides was measured in solvent mixtures of variable composition as the tetramer–hexamer equilibrium is likely influenced by differential solvation of the macrocyclic aggregates. Moreover, the resonances of the Lewis bases were indistinguishable from those in their spectra acquired from the pure compounds. These observations suggest that the integrity of the macrocyclic aggregates of iso-tellurazole N-oxides is not compromised by the Lewis bases, including the N-heterocyclic carbene **3**.

On the other hand, the addition of BR_3 ($\text{R} = \text{Ph}$ or F) to a solution of **1** immediately caused a colour change from pale yellow to pale orange and the corresponding products could be isolated in crystalline form. Their ^1H NMR resonances are shifted to higher frequency (Fig. S2†); mass spectrometry, and single-crystal X-ray diffraction confirmed the identity of the products as the O-bonded borane adducts **1-BR₃**.

In sharp contrast to **1**, **1-BR₃** ($\text{R} = \text{Ph}$, F) readily reacted with Lewis bases. Upon mixing, an immediate colour change from orange to pale yellow was accompanied by marked changes in the ^1H NMR spectra. For example, the methyl resonances of **1-BR₃** shift to lower frequency after the addition of DMAP (Fig. S3†). However, pure products could not be isolated from **1-BPh₃**. From **1-BF₃**, it was possible to isolate DMAP-**1-BF₃** and BF_3 -**1-4,4'-bipy-1-BF₃** as crystalline solids, the latter as an example of a 1 : 2 adduct with a bidentate base. It was also possible to obtain an adduct by the addition of one equivalent of **1** to **1-BF₃**, the product **1-1-BF₃** is effectively a borane capped version of the dimer of an iso-tellurazole N-oxide.

The annulated iso-tellurazole N-oxide **2** also reacts with BF_3 but pure **2-BF₃** could not be crystallised, instead crystals of $\text{CH}_3\text{CN-2-BF}_3$ were obtained from acetonitrile solutions. This adduct of acetonitrile with **2-BF₃** is more soluble than pure **2** and the acetonitrile molecule was readily displaced by other bases. These properties permitted the preparation of $\text{Ph}_3\text{P-2-BF}_3$, and **3-2-BF₃**. The latter is very sensitive to moisture; attempts to isolate the analogue from **1** yielded a solid that quickly transformed into an adduct of O^{2-} and crystallised as $[\text{3-H}]_2^+[\text{BF}_3\text{-1-O-1-BF}_3]^{2-}$ and is also very moisture sensitive.

X-ray diffraction structures

Details of the crystallographic determination of the structures of **1-BR₃** ($\text{R} = \text{Ph}$, F) are provided in the ESI.† The most relevant molecular dimensions are compiled in Table 1. There are no structurally characterised examples in literature of non-aggregated iso-tellurazole oxides other than protonated products such as X-1-H ($\text{X} = \text{Cl}$, Br),¹⁴ even in that case the tellurium atom is bound to the halide anion. In

Table 1 Selected bond distances and angles, and torsion angles of 1-BR₃ (R = Ph, F)

| | 1-BPh ₃ | 1-BF ₃ |
|---------------------------|--------------------|-------------------|
| Bond distances (Å) | | |
| Te1–C1 | 2.081(2) | 2.076(4) |
| Te1–N1 | 2.063(2) | 2.072(3) |
| N1–O1 | 1.355(2) | 1.372(4) |
| O1–B1 | 1.571(3) | 1.480(5) |
| C1–C2 | 1.364(3) | 1.354(5) |
| C2–C3 | 1.425(3) | 1.430(6) |
| C3–N1 | 1.320(3) | 1.313(5) |
| Bond angles (°) | | |
| N1–Te1–C1 | 79.63(8) | 79.2(1) |
| O1–N1–Te1 | 124.2(1) | 123.9(2) |
| Torsion angles (°) | | |
| Te1–N1–O1–B1 | 72.5(2) | 46.0(4) |
| C1–Te1–N1–O1 | 175.6(2) | 173.1(3) |

this regard, the borane adducts 1-BPh₃, and 1-BF₃ display inter- and intra-molecular contacts to C_{BPh} and F atoms (Fig. 1) shorter than the sums of van der Waals radii. The B–O bond is longer 1-BPh₃ (1.571(3) Å) than in 1-BF₃ (1.480(5) Å). Compared to previous measurements for the heterocycles,^{13,15} the Te–C distances, 2.081(2) and 2.076(4) Å, are unchanged but the Te–N distances, 2.063(2) and 2.072(3) Å, are longer by more than 0.1 Å and the C–Te–N angles, 79.63(8)° and 79.2(1)°, are wider by more than 2°.

The crystallographic analyses confirmed that in the other compounds the bases do form Te[⋯]LB chalcogen bonds with the iso-tellurazole heterocycle. All crystallographic details are included in the ESI;† selected molecular dimensions are compiled in Table 2 and ORTEPs are presented in Fig. 2.

The geometry around the chalcogen atoms is approximately T-shaped but the N–Te[⋯]LB ranges only from 162.44(5)° in CH₃CN-2-BF₃ to just 168.48(6)° in Ph₃P-2-BF₃. Scaled to the sum of van der Waals radii, the length of the chalcogen bonds varies from 58% in 3-2-BF₃ to 68% in CH₃CN-2-BF₃ and Ph₃P-2-BF₃. In most cases there is an inverse correlation between the distance from Te to N and LB. In 3-2-BF₃ and especially in [BF₃-1-O-1-BF₃]²⁻ the Te1[⋯]LB distance is nearly equal to the sum of covalent radii and the Te–N1 distance is so long (>2.4 Å) that the roles of N

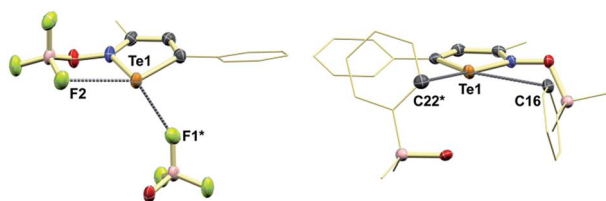


Fig. 1 ORTEP (75%) detail of the crystal structures of 1-BR₃ (R = Ph, F). Te1[⋯]C16 3.253 Å, Te1[⋯]C22* 3.445 Å, cf. Σr_{vdW} = 3.76 Å. Te1[⋯]F2 3.253 Å, Te1[⋯]F1* 3.445 Å, cf. Σr_{vdW} = 3.53 Å. All hydrogens are omitted and portions of the structure are simplified for clarity.

Table 2 Selected bond distances and angles from the adducts formed by 1-BF₃ and 2-BF₃ with Lewis bases

| | CH ₃ CN-2-BF ₃ | DMAP-1-BF ₃ | BF ₃ -1-4,4'-bipy-1-BF ₃ | Ph ₃ P-2-BF ₃ | 3-2-BF ₃ | 1-1-BF ₃ | [BF ₃ -1-O-1-BF ₃] ²⁻ |
|---|--------------------------------------|------------------------|--|-------------------------------------|---------------------|---------------------|---|
| Bond distances (Å) | | | | | | | |
| Te1...LB ^a | 2.463(2) | 2.251(3), 2.262(3) | 2.332(2) | 2.6072(9) | 2.179(9) | 2.194(6) | 2.014(3) |
| % Σ <i>r</i> _{cov} | 118% | 108%, 108% | 112% | 106% | 103% | 108% | 99% |
| % Σ <i>r</i> _{vdw} | 68% | 62%, 63% | 65% | 68% | 58% | 61% | 56% |
| Te1-C1 | 2.097(1) | 2.101(3), 2.105(3) | 2.109(3) | 2.126(3) | 2.15(1) | 2.112(9) | 2.099(4), 2.106(6) |
| Te1-N1 | 2.156(2) | 2.266(3), 2.267(3) | 2.219(2) | 2.409(2) | 2.489(8) | 2.221(5) | 2.409(3), 2.488(4) |
| N1-O1 | 1.378(2) | 1.376(3), 1.379(4) | 1.378(2) | 1.367(3) | 1.34(1) | 1.374(9) | 1.386(5), 1.397(5) |
| O1-B1 | 1.494(2) | 1.482(5), 1.490(5) | 1.498(3) | 1.485(5) | 1.44(2) | 1.50(1) | 1.484(8), 1.489(6) |
| C1-C2 | 1.414(2) | 1.348(4), 1.356(4) | 1.350(3) | 1.411(4) | 1.46(2) | 1.35(1) | 1.338(6), 1.354(6) |
| C2-C3 | 1.436(2) | 1.449(4), 1.456(4) | 1.441(3) | 1.458(4) | 1.39(2) | 1.43(1) | 1.448(7), 1.450(6) |
| C3-N1 | 1.293(2) | 1.298(4), 1.299(4) | 1.302(3) | 1.280(4) | 1.29(2) | 1.29(1) | 1.285(7), 1.297(6) |
| Te2 ^b -C11 ^b | | | | | | 2.089(9) | |
| Te2 ^b -N2 ^b | | | | | | 2.082(6) | |
| N2 ^b -O2 ^b | | | | | | 1.346(9) | |
| C11 ^b -C12 ^b | | | | | | 1.36(1) | |
| C12 ^b -C13 ^b | | | | | | 1.43(1) | |
| C13 ^b -N2 ^b | | | | | | 1.32(1) | |
| Bond angles (°) | | | | | | | |
| N1-Te1-LB ^a | 162.44(5) | 164.0(1), 165.2(1) | 163.37(8) | 168.48(6) | 167.7(3) | 165.8(2) | 166.0(1), 165.3(1) |
| N1-Te1-C1 | 77.70(5) | 75.6(1) | 76.10(8) | 74.3(1) | 74.7(3) | 76.2(3) | 72.3(1), 72.7(2) |
| C1-Te1-LB ^a | 85.34(6) | 88.7(1) | 87.29(8) | 94.78(8) | 93.0(4) | 90.4(3) | 92.6(2), 93.9(1) |
| O1-N1-Te1 | 125.7(1) | 129.2(2), 129.4(2) | 129.0(1) | 130.4(2) | 133.1(6) | 128.0(5) | 131.8(3), 133.9(2) |
| N2 ^b -Te2 ^b -C11 ^b | | | | | | 79.0(3) | |
| O2 ^b -N2 ^b -Te2 ^b | | | | | | 124.2(5) | |

Table 2 (Contd.)

| | CH ₃ CN-2-BF ₃ | DMAP-1-BF ₃ | BF ₃ -1-4,4'-bipy-1-BF ₃ | Ph ₃ P-2-BF ₃ | 3-2-BF ₃ | 1-1-BF ₃ | [BF ₃ -1-O-1-BF ₃] ¹²⁻ |
|--|--------------------------------------|------------------------|--|-------------------------------------|---------------------|---------------------|--|
| Torsion angles (°) | | | | | | | |
| Te1-N1-O1-LB ^a | 51.9(2) | 10.6(4), 30.2(4) | 24.6(3) | 25.1(3) | 15(1) | 14.9(9) | 13.7(5), 34.8(5) |
| LB ^a -Te1-N1-O1 | 157.8(2) | 168.8(3), 177.6(3) | 177.8(2) | 156.8(2) | 179(1) | 158.4(7) | 164.6(4), 173.9(4) |
| C1-Te1-N1-O1 | 173.2(1) | 174.4(3), 179.0(3) | 174.9(2) | 176.6(2) | 179(1) | 177.5(7) | 170.6(4), 176.7(4) |
| C11 ^b -Te2 ^b -N2 ^b -O2 ^b | | | | | | 179.7(6) | |

^a LB denotes the atom of the chalcogen-bond acceptor atom, *i.e.* the atom of the Lewis base linked to tellurium. ^b Denotes atoms in the molecule of **1** acting as a Lewis base in **1-1-BF₃**.

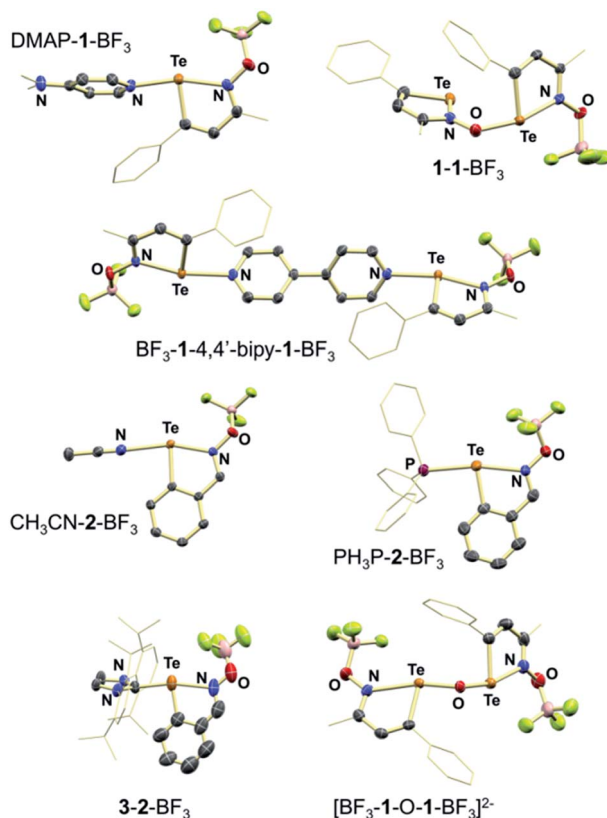


Fig. 2 ORTEP (75%) representation of the compounds structurally characterised. All hydrogens are omitted and portions of the structure are simplified for clarity.

and LB are practically swapped, N1 can be regarded as the chalcogen bond acceptor atom. However, $\text{Ph}_3\text{P-2-BF}_3$ stands out having one of the longest Te–N1 distances with a Te–P distance about 68% of the sum of van der Waals radii.

The case of 1-1-BF_3 is particularly interesting as it features two iso-tellurazole-oxide moieties in two different roles, one as chalcogen-bond acceptor and the other as the donor; alternatively, they could be identified as the Lewis base and the Lewis acid. Indeed, the bond distances and angles around tellurium in the terminal heterocycle are comparable to those observed in 1-BR_3 ($\text{R} = \text{Ph}, \text{F}$) and in the middle ring the structural parameters are similar to the measurements from the other Lewis base adducts.

Table 3 Maximum electrostatic potential on the 10^{-3} a.u. isodensity surface and frontier orbital energies of **1** and **2** and their borane adducts

| | 1 | 1-BPh₃ | 1-BF₃ | 2 | 2-BF₃ |
|--|----------|--------------------------|-------------------------|----------|-------------------------|
| V_{max} (a.u.) $\times 10^{-2}$ | 3.4 | 4.7 | 4.7 | 5.3 | 8.6 |
| V_{max} (kJ mol ^{−1}) | 89.3 | 94.5 | 147.0 | 139.6 | 225.8 |
| E_{LUMO} (eV) | −3.03 | −3.03 | −3.31 | −3.30 | −3.55 |

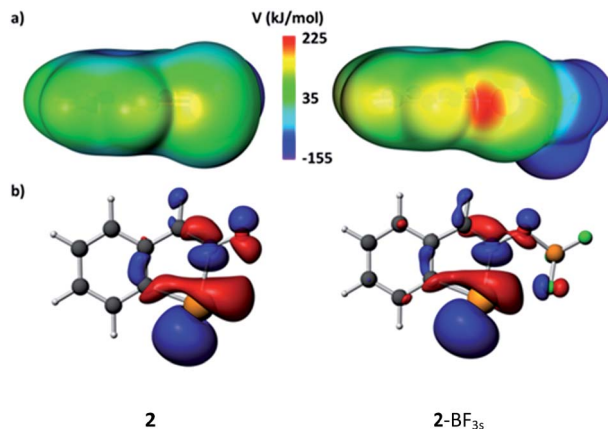


Fig. 3 (a) Maps of electrostatic potential on the isosurface of 10^{-3} a.u. electron density for 2 and 2-BF₃. (b) LUMO of 2 and 2-BF₃ plotted at 0.04 a.u.

Computational analysis

DFT calculations (PBE-D3, ZORA, TZ2P) were carried out to assess the strength of the interactions of the Lewis bases with the borane adducts of iso-tellurazole N-oxides. In the first instance, the impact of borane binding on the electron acceptor abilities of 1 and 2 was evaluated by its effect on the σ holes and the LUMO energies of these molecules; the results are compiled in Table 3 and are depicted graphically for 2 and 2-BF₃ in Fig. 3. The maps of electrostatic potential and the composition of the LUMO both indicate that the preferred point of

Table 4 Energy decomposition analysis, degree of charge transfer (Hirschfeld), and the Te \cdots LB bcp densities for the interaction of Lewis bases with 1-BF₃ and 2-BF₃. All energy values are in kJ mol⁻¹ unless otherwise stated

| | CH ₃ CN- 2-BF ₃ | DMAP- 1-BF ₃ | BF ₃ -1-4,4'- bipy-1-BF ₃ | Ph ₃ P- 2-BF ₃ | 3-2-BF ₃ | 1-1-BF ₃ | [BF ₃ -1-O- 1-BF ₃] ²⁻ |
|---|--|----------------------------|--|---|---------------------|---------------------|---|
| E_{elstat} | -81.59 | -233.26 | -163.20 | -266.91 | -463.09 | -290.06 | -344.98 |
| E_{Pauli} | 96.48 | 304.16 | 224.45 | 398.71 | 644.48 | 448.61 | 635.65 |
| E_{steric} | 14.89 | 70.90 | 61.25 | 131.8 | 181.39 | 158.55 | 290.68 |
| E_{orbital} | -50.67 | -147.51 | -105.28 | -229.94 | -351.08 | -246.67 | -1072.72 |
| $E_{\text{dispersion}}$ | -6.06 | -22.38 | -28.15 | -30.11 | -55.34 | -27.47 | -29.37 |
| $E_{\text{Te}\cdots\text{LB}}$ | -41.84 | -98.99 | -72.18 | -128.25 | -225.03 | -115.59 | -811.41 |
| $E_{\text{preparation}}$ | 2.81 | 19.57 | 22.31 | 37.76 | 54.64 | 28.39 | 477.49 |
| E_{total} | -39.03 | -79.42 | -49.87 | -90.49 | -170.39 | -87.20 | -333.92 |
| $\Delta ZPE \times 10^{-2}$ | 2.54 | 4.80 | 3.10 | 2.80 | 4.20 | 2.66 | 4.24 |
| [eV] | | | | | | | |
| ΔH | -36.24 | -77.16 | -49.26 | -89.35 | -165.29 | -86.94 | -334.35 |
| ΔS | -130.59 | -215.84 | -244.94 | -213.26 | -205.39 | -223.61 | -246.43 |
| [J mol ⁻¹ K ⁻¹] | | | | | | | |
| $\Delta G_{273.15\text{ K}}$ | 2.69 | -12.81 | 23.77 | -25.74 | -104.05 | -20.26 | -260.88 |
| Δq (a.u.) | 0.07 | 0.20 | 0.14 | 0.24 | 0.27 | 0.07 | 0.69 |
| $\rho_{\text{BCP}}(\text{Te}\cdots\text{LB})$ | 2.72 | 5.44 | 4.38 | 5.69 | 7.77 | 6.72 | 10.9 |
| (a.u.) $\times 10^{-2}$ | | | | | | | |

attachment of a base is not collinear with the Te–N bond, in agreement with the observations. According to the calculations, binding of BF₃ increases the maximum of potential at the σ holes by more than 60% and stabilizes the LUMO by at least 0.25 eV. The effect of BPh₃ on **1** is smaller but not negligible.

The energetic contributions to the interaction of Lewis bases with 1-BF₃ and 2-BF₃ were analysed under the Ziegler–Rauk transition-state approach,^{21–23} the details of which are discussed elsewhere.¹⁵ Under this scheme the total interaction (E_{total}) is the combination (eqn (1)) of the electrostatic interaction (E_{elstat}), Pauli repulsion (E_{Pauli}) and orbital interaction (E_{orbital}) supplemented by ($E_{\text{dispersion}}$) and geometric distortion ($E_{\text{preparation}}$) contributions. The sum of electrostatic and Pauli repulsion is called the total steric interaction (E_{steric}) and quantifies the electronic interaction without polarization or covalency. All calculated contributions are compiled in Table 4. For the 1 : 2 adducts, the analyses refer to the interactions between BF₃–1-4,4'-bipy and 1-BF₃, and between [BF₃–1-O]^{2–} and 1-BF₃.

$$\begin{aligned} E_{\text{total}} &= E_{\text{elstat}} + E_{\text{Pauli}} + E_{\text{orbital}} + E_{\text{dispersion}} + E_{\text{preparation}} \\ &= E_{\text{steric}} + E_{\text{orbital}} + E_{\text{dispersion}} + E_{\text{preparation}} \\ &= E_{\text{Te}\cdots\text{LB}} + E_{\text{preparation}} \end{aligned} \quad (1)$$

In general, a weak long Te[⋯]LB chalcogen bond would be predominantly controlled by the electrostatic interaction between the LB electrons and the σ hole on the chalcogen. As the attractive interaction becomes stronger, the distance decreases and the molecules become increasingly polarized until orbital mixing (covalency) ensues, further strengthening the Te[⋯]LB link. Therefore, it is reasonable to regard the lengthening of the bond opposite to the σ -hole interaction as an indicator of strength. The total energies of interaction, degrees of electron transfer and Atoms-In-Molecules (AIM) electron densities at the bond critical point (ρ_{bcp}) seem to agree with such qualitative arguments. Being the stronger bases, the carbene **3** and [BF₃–1-O]^{2–} give the largest energies of interaction and bcp densities. However, in spite of the similarities in all the energetic contributions to the Te[⋯]LB interactions in Ph₃P–2-BF₃ and 1-1-BF₃ the effect of the phosphine and the iso-tellurazole N-oxide on the Te–N1 distance is very different.

Experimental

Materials and methods

Organic solvents were purified either by distillation over the appropriate dehydrating agents under nitrogen or using an Innovative Technology purification system. Compounds **1** (ref. 13) and **2** (ref. 15) were prepared as previously described. The following chemicals were used as received from the commercial suppliers: *N,N'*-bis(2,6-diisopropyl-phenyl)imidazol-2-ylidene (Strem), DMSO-*d*₆ (Aldrich), triphenylborane (Strem). 4-Dimethylaminopyridine (Aldrich), triphenylphosphine (Aldrich), and 4,4'-bipyridine (Aldrich) were recrystallized from anhydrous toluene and sublimed under vacuum. Combustion elemental analyses were carried out by the London Metropolitan University elemental analysis service (London, United Kingdom).

Syntheses

All compounds were prepared by mixing the reagents at room temperature under an atmosphere of nitrogen. Proportions, work up and characterization are

described below. The ^{125}Te NMR resonance could not be observed in many cases due to limited solubility of the samples.

1-BF₃

3-Methyl-5-phenyl-1,2-tellurazole N-oxide (**1**, 100 mg, 0.35 mmol), 0.81 M BF₃·Et₂O (0.43 mL, 0.35 mmol), chloroform (1.15 g). The product was recrystallized from chloroform, centrifuged and dried under vacuum. Yield 92%. ^1H NMR (600 MHz, CD₂Cl₂, δ ppm): 7.58 (s, 1H); 7.56–7.49 (m, 3H); 7.45–7.42 (m, 2H); 2.73 (s, 3H). ^{13}C NMR (600 MHz, CD₂Cl₂, δ ppm): 169.76 (s, 1C); 169.25 (s, 1C); 135.53 (s, 1C); 132.03 (s, 1C); 130.30 (s, 2C); 127.64 (s, 2C); 123.01 (s, 1C); 18.63 (s, 1C). ^{125}Te NMR (600 MHz, CD₂Cl₂, δ ppm): 2116.47. Mp: 175.5–178.2 °C. Elemental anal. calcd C₁₀H₉BF₃NOte: C 33.87, H 2.56, N 3.95; found: C 33.70, H 2.38, N 3.98.

1-BPh₃

3-Methyl-5-phenyl-1,2-tellurazole N-oxide (**1**, 100 mg, 0.35 mmol), BPh₃ (84.7 mg, 0.35 mmol), chloroform (1.15 g). The product was recrystallized in a mixture of chloroform : hexanes (1 : 2 v/v), centrifuged and dried under vacuum. Yield 79%. ^1H NMR (600 MHz, 19.2 mg in 0.8 mL CD₂Cl₂, δ ppm): 7.54–7.52 (m, 6H); 7.43–7.32 (m, 4H); 7.26–7.22 (m, 8H); 7.19–7.17 (m, 3H); 2.65 (s, 3H). ^{13}C NMR (600 MHz, 19.2 mg in 0.8 mL CD₂Cl₂, δ ppm): 166.47 (s, 1C); 164.95 (s, 1C); 136.88 (s, 3C); 134.99 (s, 6C); 134.59 (s, 1C); 130.53 (s, 3C); 129.58 (s, 2C); 128.14 (s, 1C); 127.92 (s, 6C); 126.18 (s, 2C); 122.50 (s, 1C); 19.13 (s, 1C). Mp: 115.2–118.2 °C.

CH₃CN-2-BF₃

Benzo-1,2-tellurazole 2-oxide (**2**, 100 mg, 0.405 mmol) in acetonitrile (2 mL), 0.81 M BF₃·Et₂O (0.5 mL, 0.405 mmol) in chloroform (1 mL). The mixture was stirred for 1 h and the product was centrifuged and dried under vacuum. Yield 94%. ^1H NMR (600 MHz, CD₂Cl₂, δ ppm): 9.09 (s, 1H); 8.11 (d, 1H); 8.01 (d, 1H); 7.60 (dt, 1H); 7.54 (dt, 1H); 2.13 (s, 3H). ^{13}C NMR (600 MHz, CD₂Cl₂, δ ppm): 155.5 (s, 1C); 139.8 (s, 1C); 132.3 (s, 1C); 131.8 (s, 1C); 131.4 (s, 1C); 131.4 (s, 1C); 128.2 (s, 1C); 117.2 (s, 1C); 2.2 (s, 1C). Mp: 134.1–136.2 °C. Elemental anal. calcd C₉H₈·BF₃N₂Ote: C 30.40, H 2.27, N 7.88; found: C 30.52, H 2.19, N 8.02.

DMAP-1-BF₃

1-BF₃ (38.4 mg, 0.11 mmol) in dichloromethane (1.66 g), 4-dimethylaminopyridine (20.2 mg, 0.16 mmol) in dichloromethane (0.50 g). The product was precipitated with hexanes, centrifuged and dried under vacuum. Yield 98%. ^1H NMR (600 MHz, 10.2 mg in 0.8 mL CD₂Cl₂, δ ppm): 7.77 (s, 2H); 7.14 (s, 1H); 7.10 (s, 5H); 6.21 (s, 2H); 3.01 (s, 6H); 2.37 (s, 3H). ^{13}C NMR (600 MHz, 10.2 mg in 0.8 mL CD₂Cl₂, δ ppm): 161.31 (s); 155.29 (bs); 148.52 (bs); 140.19 (s); 129.12 (s); 128.06 (s); 127.19 (s); 107.40 (s), 39.70 (bs), 17.00 (s). Mp: 152.4–155.0 °C. Elemental anal. calcd C₁₇H₁₉BF₃N₃Ote: C 42.83, H 4.02, N 8.81; found: C 42.94, H 3.85, N 8.89.

BF₃-1-4,4'-bipy-1-BF₃

1-BF₃ (45.4 mg, 0.13 mmol) in dichloromethane (1.8 g), 4,4'-bipyridine (10 mg, 0.064 mmol). The product was precipitated with hexanes, centrifuged and dried

under vacuum. Yield 98%. ^1H NMR (600 MHz, CD_2Cl_2 , δ ppm): 8.53 (d, 4H); 7.43 (d, 4H); 7.39 (s, 2H); 7.29–7.27 (m, 10H); 2.60 (s, 6H). ^{13}C could not be measured due to low solubility. Mp: 233.6–235.0 °C. Elemental anal. calcd $\text{C}_{30}\text{H}_{26}\text{B}_2\text{F}_6\text{N}_4\text{O}_2\text{Te}_2$: C 41.64, H 3.03, N 6.47; found: C 41.46, H 3.15, N 6.39.

2[3-*H*]-[BF₃-1-O-1-BF₃]

1-BF₃ (10 mg, 0.028 mmol) in benzene-*d*₆ (2 g), 1,3-bis(2,6-diisopropylphenyl)-1,3-dihydro-2*H*-imidazol-2-ylidene (**3**, 10.8 mg, 0.028 mmol). The product was centrifuged and dried under vacuum. Yield 80%. ^1H NMR (600 MHz, CD_2Cl_2 , δ ppm): 8.65 (s, 2H); 7.73 (s, 4H); 7.64 (t, 4H); 7.42 (d, 8H); 7.33–7.12 (bm, 10H); 6.81 (bs, 1H), 6.59 (bs, 1H), 2.39 (sept, 8H); 2.04 (bs, 3H); 1.91 (bs, 3H); 1.29 (d, 24); 1.21 (d, 24H). ^{13}C NMR (700 MHz, CD_2Cl_2 , δ ppm): 145.4 (s); 137.8 (s); 132.9 (s); 129.9 (s); 129.4 (bs); 128.0 (bs); 127.6 (bs); 127.4 (bs); 126.6 (s); 125.4 (s); 125.2 (bs); 29.6 (s); 24.7 (s); 24.0 (s); 16.2 (bs). Mp: 122.5–125.6 °C. Despite the crystallographic determination, repeated attempts failed to provide a satisfactory elemental analysis due to moisture sensitivity.

Ph₃P-2-BF₃

2-BF₃ (29.8 mg, 0.084 mmol) in toluene (6.3 g), triphenylphosphine (34.2 mg, 0.130 mmol) in dichloromethane (7.3 g). The product was precipitated upon evaporation, centrifuged and dried under vacuum. Yield 95%. Note: Ph₃P-2-BF₃ appears to be partly dissociated in solution; an excess of phosphine is required for isolation. Consequently, small amounts of phosphine contaminate the product, as made evident by combustion analyses. Recrystallization attempts mostly yield the reactants. Crude yield 82%. ^1H NMR (600 MHz, 21.4 mg in 0.8 mL CD_2Cl_2 , δ ppm): 8.688 (d, 1H); 7.67–7.57 (m, 16H); 7.33 (t, 1H); 7.15 (d, 1H), 6.90 (t, 1H). ^{13}C NMR (700 MHz, CD_2Cl_2 , δ ppm): 149.7 (s, 1C); 135.1 (s, 1C); 134.7 (s, 1C); 134.2 (s, 6C); 134.1 (s, 6C); 133.7 (s, 3C); 131.4 (s, 1C); 130.6 (s, 3C); 130.2 (s, 1C); 128.0 (s, 1C); 123.9 (s, 1C). Mp: 152.1–154.2 °C.

3-2-BF₃

2-BF₃ (28.7 mg, 0.081 mmol) in dichloromethane (7.5 g), **3** (31.4 mg, 0.081 mmol) in benzene (7.5 mL). The product was precipitated by evaporation of the dichloromethane under vacuum, it was centrifuged and dried under vacuum. Yield 85%. ^1H NMR (600 MHz, 40 : 60 v/v CD_2Cl_2 : C_6D_6 , δ ppm): 8.57 (s, 1H); 7.85 (t, 2H); 7.70 (d, 1H), 7.66–7.65 (m, 5H); 7.62 (d, 1H); 7.52–7.50 (m, 3H); 2.94 (hept, 4H), 1.72 (d, 12H), 1.58 (d 12H). Mp: 260 °C (d). ^{13}C could not be observed due to low solubility. Despite the crystallographic determination, repeated attempts failed to provide a satisfactory elemental analysis due to moisture sensitivity.

1-1-BF₃

1-BF₃ (10 mg, 0.028 mmol) in benzene (2 g), **1** (8.1 mg, 0.028 mmol). The product crystalized slowly after mixing, it was centrifuged and dried under vacuum. Yield 75%. ^1H NMR (700 MHz, CD_2Cl_2 , δ ppm): 7.55 (s, 1H); 7.41–7.32 (m, 10H); 7.21 (s, 1H); 2.45 (s, 3H); 1.88 (s, 3H). ^{13}C NMR (700 MHz, CD_2Cl_2 , δ ppm): 163.4 (s, 1C); 160.2 (s, 1C); 158.1 (s, 1C); 138.0 (s, 1C); 136.9 (s, 1C); 129.9 (s, 1C); 129.2 (s, 2C); 129.1 (s, 2C); 128.8 (s, 1C); 128.3 (s, 1C); 127.9 (s, 2C), 127.3 (s, 2C), 126.9 (s, 1C),

125.0 (s, 1C); 17.0 (s, 1C), 16.4 (s, 1C). Mp: 180.1–182.0 °C. Elemental anal. calcd C₂₀H₁₈BF₃N₂O₂Te₂: C 37.45, H 2.83, N 4.37; found: C 37.48, H 2.74, N 4.41.

DFT calculations

All calculations were performed using the ADF DFT package (Version 2013.01).^{24,25} All models were optimized using the exchange–correlation functionals of Perdew, Burke, and Ernzerhof²⁶ and corrected for dispersion²⁷ with a triple- ζ all-electron basis set with two polarization functions each and applying the Zeroth Order Regular Approximation^{28–31} formalism with specially adapted basis sets. Frequency calculations were performed to ensure that each geometry was at an actual minimum in the potential energy surface and to derive the corresponding thermodynamic parameters.^{32,33}

Conclusions

The supramolecular macrocycles assembled by iso-tellurazole oxides appear to be remarkably impervious to bases as strong as N-heterocyclic carbenes. This is puzzling considering the fast equilibrium that takes place in solution between tetramers and hexamers in solution. In contrast, BR₃ (R = Ph, F) boranes yielded 1 : 1 O-bonded adducts that readily form strong chalcogen bonds with Lewis bases. In this way, it is possible to obtain new adducts and even stabilize an unusual chalcogen-bonded dimer of iso-tellurazole N-oxide. These reactions will be particularly useful in guiding the combination of iso-tellurazole N-oxides with other building blocks to build supramolecular structures beyond halogen bonding.

Acknowledgements

We gratefully acknowledge funding from the Natural Science and Engineering Research Council of Canada and the Ontario Graduate Scholarship program.

Notes and references

- 1 K. Rissanen, *CrystEngComm*, 2008, **10**, 1107–1113.
- 2 P. Metrangolo, F. Meyer, T. Pilati, G. Resnati and G. Terraneo, *Angew. Chem., Int. Ed.*, 2008, **47**, 6114–6127.
- 3 P. Metrangolo and G. Resnati, *Science*, 2008, **321**, 918–919.
- 4 K. Raatikainen and K. Rissanen, *Chem. Sci.*, 2012, **3**, 1235–1239.
- 5 A. Priimagi, M. Saccone, G. Cavallo, A. Shishido, T. Pilati, P. Metrangolo and G. Resnati, *Adv. Mater.*, 2012, **24**, OP345–OP352.
- 6 M. J. Langton, S. W. Robinson, I. Marques, V. Félix and P. D. Beer, *Nat. Chem.*, 2014, **6**, 1039–1043.
- 7 T. A. Barendt, A. Docker, I. Marques, V. Félix and P. D. Beer, *Angew. Chem., Int. Ed.*, 2016, **55**, 11069–11076.
- 8 G. E. Garrett, E. I. Carrera, D. S. Seferos and M. S. Taylor, *Chem. Commun.*, 2016, **52**, 9881–9884.
- 9 J. Qiu, D. K. Unruh and A. F. Cozzolino, *J. Phys. Chem. A*, 2016, **120**, 9257–9269.

- 10 F. Kniep, S. H. Jungbauer, Q. Zhang, S. M. Walter, S. Schindler, I. Schnapperelle, E. Herdtweck and S. M. Huber, *Angew. Chem., Int. Ed.*, 2013, **52**, 7028–7032.
- 11 S. Benz, J. López Andarias, J. Mareda, N. Sakai and S. Matile, *Angew. Chem., Int. Ed.*, 2017, **56**, 812–815.
- 12 N. K. Beyeh, F. Pan and K. Rissanen, *Angew. Chem., Int. Ed.*, 2015, **54**, 7303–7307.
- 13 P. C. Ho, P. Szydlowski, J. Sinclair, P. J. W. Elder, J. Kübel, C. Gendy, L. M. Lee, H. Jenkins, J. F. Britten, D. R. Morim and I. Vargas-Baca, *Nat. Commun.*, 2016, **7**, 11299.
- 14 P. C. Ho, L. M. Lee, H. Jenkins, J. F. Britten and I. Vargas-Baca, *Can. J. Chem.*, 2016, **94**, 453–457.
- 15 P. C.-W. Ho, J. Rafique, J. Lee, M. L. Lee, H. A. Jenkins, J. F. Britten, A. L. Braga and I. Vargas-Baca, *Dalton Trans.*, 2017, **46**, 6570.
- 16 A. F. Cozzolino, P. S. Whitfield and I. Vargas-Baca, *J. Am. Chem. Soc.*, 2010, **132**, 17265–17270.
- 17 N. A. Semenov, A. V. Lonchakov, N. A. Pushkarevsky, E. A. Suturina, V. V. Korolev, E. Lork, V. G. Vasiliev, S. N. Konchenko, J. Beckmann, N. P. Gritsan and A. V. Zibarev, *Organometallics*, 2014, **33**, 4302–4314.
- 18 N. A. Semenov, A. V. Lonchakov, N. P. Gritsan and A. V. Zibarev, *Russ. Chem. Bull.*, 2015, **64**, 499–510.
- 19 J. L. Dutton and P. J. Ragona, *Inorg. Chem.*, 2009, **48**, 1722–1730.
- 20 G. E. Garrett, G. L. Gibson, R. N. Straus, D. S. Seferos and M. S. Taylor, *J. Am. Chem. Soc.*, 2015, **137**, 4126–4133.
- 21 T. Ziegler and A. Rauk, *Theor. Chim. Acta*, 1977, **46**, 1–10.
- 22 T. Ziegler and A. Rauk, *Inorg. Chem.*, 1979, **18**, 1755–1759.
- 23 T. Ziegler and A. Rauk, *Inorg. Chem.*, 1979, **18**, 1558–1565.
- 24 G. te Velde, F. M. Bickelhaupt, E. J. Baerends, C. Fonseca Guerra, S. J. A. van Gisbergen, J. G. Snijders and T. Ziegler, *J. Comput. Chem.*, 2001, **22**, 931–967.
- 25 C. F. Guerra, J. G. Snijders, G. te Velde and E. J. Baerends, *Theor. Chem. Acc.*, 1998, **99**, 391–403.
- 26 J. P. Perdew, K. Burke and M. Ernzerhof, *Phys. Rev. Lett.*, 1996, **77**, 3865–3868.
- 27 S. Grimme, *J. Comput. Chem.*, 2006, **27**, 1787–1799.
- 28 E. van Lenthe, A. Ehlers and E.-J. Baerends, *J. Chem. Phys.*, 1999, **110**, 8943–8953.
- 29 E. Van Lenthe, R. Van Leeuwen, E. J. Baerends and J. G. Snijders, *Int. J. Quantum Chem.*, 1996, **57**, 281–293.
- 30 E. Van Lenthe, E. J. Baerends and J. G. Snijders, *J. Chem. Phys.*, 1994, **101**, 9783–9792.
- 31 E. Van Lenthe, E. J. Baerends and J. G. Snijders, *J. Chem. Phys.*, 1993, **99**, 4597–4610.
- 32 A. Bérces, R. M. Dickson, L. Fan, H. Jacobsen, D. Swerhone and T. Ziegler, *Comput. Phys. Commun.*, 1997, **100**, 247–262.
- 33 S. K. Wolff, *Int. J. Quantum Chem.*, 2005, **104**, 645–659.